Electronic Supplementary Material (ESI) for Dalton Transactions.
This journal is © The Royal Society of Chemistry 2023

Silver-based coordination polymers assembled by dithioether ligands: potential antibacterial materials despite received ideas

Quentin Gaudillat[1], Anna Krupp[2], Thibaut Zwingelstein[3], Vincent Humblot[3], Carsten Strohmann[2], Isabelle Jourdain[1], Michael Knorr[1], Lydie Viau[1*]

[a] *Institut UTINAM, UMR CNRS 6213, 16 Route de Gray, Université Franche-Comté, 25030 Besançon, France*

[b] *Anorganische Chemie, Technische Universität Dortmund, Otto-Hahn-Straße 6, 44227 Dortmund, Germany*

[c] *Université Franche-Comté, UMR CNRS 6174, Institut FEMTO-ST UMR 6174, 15B avenue des Montboucons, 25030 Besançon, France.*

Table of contents

Experimental procedure

1. Materials

$AgNO_3$, NaOH, KOH, 1,4-dichlorobut-2-yne, cyclohexanethiol, thiophenol, the culture media Mueller Hinton (MH) broth, Lysogeny broth Miller (Luria-Bertani) and PBS were commercially obtained from Acros, Alfa Aesar, Aldrich, TCI and Difco.

2. Physical Measurement and Instrumentation.

The ^{1}H and ^{13}C NMR spectra were obtained on a Bruker AVANCE 400 HD instrument. ^{1}H chemical shifts were referenced to the proton impurity of the NMR solvent and ^{13}C chemical shifts to the NMR solvent. Infrared spectra were recorded with a 2 cm^{-1} resolution on a Bruker vertex70 FTIR spectrometer using a Platinum ATR accessory equipped with a diamond crystal. Elemental analyses were performed on a Thermo Fisher Flashsmart CHNS elemental analyzer. Inductively Coupled Plasma Atomic Emission Spectrometry (ICP-AES) measurements were performed on a Radial ICAP 6500 Model, Thermo Fisher Scientific (Courtaboeuf, France).
Scanning Electron Microscopy (SEM-FEG). SEM images were recorded with a ThermoFisher Apreo S field emission gun scanning electron microscope (SEM-FEG) using high vacuum mode. MIC/2, MIC and MIC×2 concentrations of **CP1** were incubated with a 10^{7} $CFU.mL^{-1}$ *E. coli* suspension in PBS at 30°C and stirred at 90 rpm for 30 min. 10 mm × 10 mm × 2 mm stainless steel wafers were immerged in the suspensions for another 30 min and bacteria were fixed on the substrate by immersion in a 2.5% glutaraldehyde solution in PBS for 2 h. Samples were rinsed 3 times in PBS, dehydrated progressively in PBS - ethanol solutions (EtOH 25%, EtOH 50%, EtOH 75%, EtOH 96%, absolute EtOH) for 5 min each and dried under laminar flow. The samples were fixed on an alumina SEM support with a carbon adhesive tape and were observed without metallization. In-chamber secondary electron detector was used in standard mode (Everhart Thornley Detector, ETD) to detect only secondary electrons. The accelerating voltages were comprised between 3 and 5 kV, and the working distance was around 10 mm. At least ten to 15 different locations were analyzed on each surface.

3. Ligands and CP syntheses

The dithioether ligands 1,4-bis(phenylthio)but-2-yne **L1** and 1,4-bis(cyclohexylthio)but-2-yne **L2** were synthesized in one step according to a slightly modified procedure described by Murray[1] *i.e* by reaction of *in-situ* generated phenylthiolate (or cyclohexylthiolate) with 1,4-dichlorobutyne.

Synthesis of L1

To a solution of NaOH (1.26 g, 32 mmol) in 70 mL ethanol was added 3.4 g of thiophenol (31 mmol). After cooling down to 0°C, 1.89 g of 1,4-dichlorobut-2-yne (15 mmol) was slowly added. The mixture was stirred overnight at room temperature. The solvent was evaporated to 20 mL and the mixture was kept one hour at 4°C. The precipitate was filtrated and washed with water until silver nitrate test indicated that NaCl was fully removed, then dried with methanol. The product was obtained as a yellowish solid (3.46 g, 87%). ^{1}H NMR (400.1 MHz, $CDCl_3$): δ = 7.39 (m, 4H, C<u>H</u>$_{ortho}$), 7.28 (m, 4H, C<u>H</u>$_{meta}$), 7.22 (m, 2H, C<u>H</u>$_{para}$), 3.61 (s, 4H, C<u>H</u>$_2$S).^{13}C{^{1}H} NMR (100.6 MHz, $CDCl_3$): δ = 135.4 (<u>C</u>$_{ipso}$), 130.0 (<u>C</u>H$_{ortho}$), 129.1 (<u>C</u>H$_{meta}$), 126.9 (<u>C</u>H$_{para}$), 79.4 (C≡C), 23.2 (S<u>C</u>H$_2$). IR (ATR): 3048 (w), 2937 (w), 2908 (w), 1580 (m), 1477 (m), 1438 (m), 1399 (m), 1235 (m), 1087 (w), 1070 (w), 1021 (m), 731 (s), 704 (m), 686 (s), 496 (m), 470 (m) cm^{-1}. mp : 54°C.

Synthesis of L2

To a solution of KOH (5.9 g, 105 mmol) in 100 mL ethanol was added 13 mL of cyclohexanethiol (106 mmol). After 1h of stirring, 4.88 mL of 1,4-dichlorobut-2-yne (50 mmol, 1 eq) were slowly added. The mixture was stirred overnight at room temperature and then refluxed for two hours. Formed KCl salts were filtered, and the solvent was evaporated. The crude product was dissolved in 50 mL CH_2Cl_2, the organic layer was washed with water (3 × 20 mL), dried over sodium sulfate, and the solvent was removed under vacuum. The product was obtained as an orange oil (12.021 g, 86%). NMR analyses revealed sufficient purity to be used without further purification. ^{1}H NMR (400.1 MHz, $CDCl_3$): δ = 3.23 (s, 4H, C<u>H</u>$_2$S), 2.82 (m, 2H, CH $_{cyclohexyl}$), 1.92 (m, 4H, CH$_{2\ cyclohexyl}$), 1.71 (m, 4H, CH$_{2cyclohexyl}$), 1.56 (m, 2H, CH$_{2\ cyclohexyl}$), 1.22 (m, 10H, CH$_{2cyclohexyl}$). ^{13}C{^{1}H} NMR (100.6 MHz, $CDCl_3$): δ = 79.0 (C≡C), 43.2 (S<u>C</u>H), 33.1 (SCH<u>C</u>H$_2$), 26.0 (SCHCH$_2$<u>C</u>H$_2$), 25.9 (SCHCH$_2$CH$_2$<u>C</u>H$_2$), 18.2 (C≡C<u>C</u>H$_2$S). IR (ATR): 2924 (s), 2850 (m), 1447 (m), 1410 (w), 1340 (w), 1264 (w), 1232 (w), 1204 (w), 998 (m), 886 (w), 819 (w), 739 (w), 700 (w) cm^{-1}.

Synthesis of CP1

To a methanol solution of $AgNO_3$ (572 mg, 2 mmol) (10mL) was added a solution of **L1** (270 mg, 1 mmol) in 5 mL of chloroform. A white precipitate appeared instantly. The mixture was stirred for 2 h and the resulting precipitate was filtered. Crystals suitable for X-ray analysis were obtained by slow evaporation of the supernatant. (406 mg, 67%). IR (ATR): 3054 (w), 2974 (w), 1471 (w), 1440 (m), 1415 (m), 1284 (s), 1233 (m), 1070 (w), 1033 (m), 1021 (m), 999 (m), 816 (m), 749 (s), 686 (s), 491 (s), 456 (s) cm^{-1}. Anal. Calc for $C_{16}H_{14}Ag_2N_2O_6S_2$ (610.15): %C 31.50, %H 2.31, %N 4.59, %S 10.51; found: %C 31.21, %H 2.21, %N 4.81, %S 10.25.

Synthesis of CP2

To an acetonitrile solution of $AgNO_3$ (850 mg, 5 mmol) (20 mL) was added a solution of **L2** (564 mg, 2 mmol) in 5 mL of acetonitrile. A precipitate appeared after a few minutes of stirring. The mixture was stirred for 2 h and the resulting precipitate was filtered. A small amount of the powder was dissolved in hot acetonitrile. After several days, crystals suitable for X-ray analysis appeared (532 mg, 59%). IR (ATR): 2925 (s), 2851 (m), 1447 (m), 1413 (m), 1329 (s), 1264 (w), 1240 (w), 1115 (m), 1039 (m), 1026 (m), 995 (m), 888 (w), 817 (m), 690 (m), 624 (m), 509 (w) cm^{-1}. Anal. Calc for $C_{16}H_{26}AgNO_3S_2$ (452.37): %C 42.48, %H 5.79, %N 3.10, %S 14.18; found: %C 42.34, %H 5.58, %N 2.97, %S 13.75 %.

4. Antibacterial activity

Bacterial strains and growth conditions

Microbiological experiments were conducted with Gram-negative *Escherichia coli (E. coli* ATCC 25922) and Gram-positive *Staphylococcus aureus* (*S. aureus* ATCC 25923). Bacteria were stored at -80°C. Before the experiments, they were incubated overnight (OVN) at 30°C on Lysogeny Broth (Miller-LB, 20 $g.L^{-1}$) agar plate for *E. coli* and at 37°C on Mueller-Hinton (MH, 25$g.L^{-1}$) agar (15g/L) plate for *S. aureus*. Then, a liquid pre-culture was prepared with one colony of *E. coli* or *S. aureus* in LB or MH media, respectively, and stirred overnight (90 rpm) at 30°C or 37°C. Bacterial concentration in liquid culture was estimated via UV-Vis spectroscopy (UV-2450 Shimadzu spectrophotometer) at 620 nm using a calibration curve. At this stage, the initial bacterial concentration is close to 10^9 $CFU.mL^{-1}$.

Minimal Inhibition Concentration (MIC) measurements

MICs values were determined by the two-fold dilution method. Experiments were performed in 96-well microplates as triplicate in culture media (LB for *E. coli* and MH for *S. aureus*), with an initial bacterial concentration of approximately 10^6 CFU.mL^{-1}. The highest concentrations were prepared according to the following: $AgNO_3$ in distilled water, ligands in water/acetonitrile (94/6 % v/v) and CPs as suspensions in culture media. We previously checked that these concentrations of acetonitrile did not detrimentally affect bacterial growth. These concentrations were then twofold serially diluted with broth. After overnight incubation at 30°C/37°C, the turbidity of the samples was assessed. MICs were determined as the lowest concentration of the compound with no visible bacterial growth. Turbidity measurements were confirmed by absorbance measurements using a microplate reader. In the case of CPs, extra experiments were carried out to confirm the results. In these cases, different concentrations of CPs suspensions were prepared directly in culture media. Sterility control (culture broth only), growth control (culture broth with bacteria) and death control (culture broth with bacteria and 50% ethanol) assessed the quality of each experiment. MICs determination was performed in triplicate.

Minimum Bactericidal Concentration (MBC) measurements

MBCs determination against *E. coli* was performed by traditional dilution/counting carried out in triplicate on LB agar plates. The plates were incubated at 30 °C overnight before enumeration. MBCs values were taken when ≥99.99% of the initial bacteria were killed (*i.e*. ≥3 log10 CFU.mL^{-1}).

Time-killing assays

Exponentially growing of *E. coli* in LB was harvested by centrifugation (5000×g, 5 min, 4°C), washed once with PBS, suspended and diluted in PBS to obtain a concentration of 10^6 CFU.mL^{-1}. This bacterial suspension was incubated at 30°C with **CP1** or **CP2** at 1 or 10 $\mu g\ Ag.mL^{-1}$. Aliquots of 100 µL were withdrawn at different times, diluted in LB, and spread onto LB + agar (20 g/L + 15 g/L) plates using Interscience EasySpiral automatic inoculator. After overnight incubation at 30°C, the CFUs were enumerated with a Interscience Colony Counter Scan 300. Controls were run without CP and experiments were performed in duplicate.

5. Silver release

CPs were suspended in 200 mL PBS at 30°C and stirred at 90 rpm. For each indicated time, 15 mL of the solution were sampled and replaced by fresh PBS to maintain the total volume constant. Ag concentrations in solution were determined in triplicate using Inductively Coupled Plasma Atomic Emission Spectrometry (ICP-AES). Quality control was achieved by analyzing a standard solution every 10 samples and the detection limit was 3.64 $\mu g.L^{-1}$.

6. X-ray Cristallography

X ray powder patterns were obtained at 295 K on a D8 Advance Bruker diffractometer using Ni-filtered K-α radiation. The crystal structures of compounds **CP1** and **CP2** were determined using the *Bruker D8 Venture* four-circle diffractometer equipped with a *PHOTON II* CPAD detector by *Bruker AXS GmbH*. The X-ray radiation was generated by the *IμS* microfocus source [and *IμS 3.0* microfocus source for **CP2**] Mo (λ = 0.71073 Å) from *Incoatec GmbH* equipped with HELIOS mirror optics and a single-hole collimator by *Bruker AXS GmbH*. The selected single crystal of **CP1** and **CP2** were covered with an inert oil (perfluoropolyalkyl ether) and mounted on the *MicroMount* from *MiTeGen*. The APEX 4 Suite (v.2021.10-0) software integrated with SAINT (integration) and SADABS (adsorption correction) programs by *Bruker AXS GmbH* were used for data collection. The processing and finalization of the crystal structure were performed using the Olex2 program.[2] The crystal structures were solved by the ShelXT[3] structure solution program using the Intrinsic Phasing option, which were further refined by the ShelXL[4] refinement package using Least Squares minimization. The non-hydrogen atoms were anisotropically refined. All hydrogen atoms were located on the Difference-Fourier-Map and refined independently in every structure. The crystallographic data for the structures of **CP1** and **CP2** have been published as supplementary publication number 2237576 (**CP1**) and 2237575 (**CP2**) in the Cambridge Crystallographic Data Centre. A copy of these data can be obtained for free by applying to CCDC, 12 Union Road, Cambridge CB2 IEZ, UK, fax: 144-(0)1223-336033 or e-mail: deposit@ccdc.cam.ac.uk.

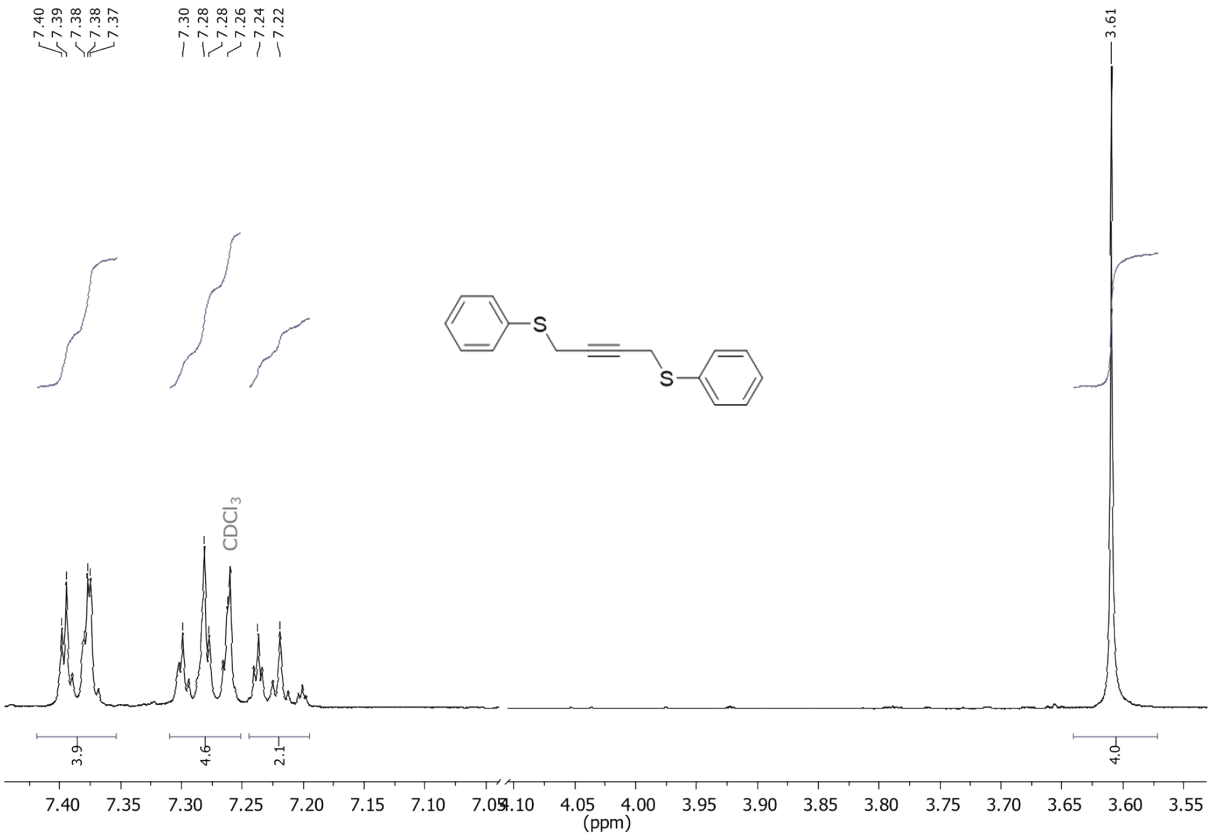

Fig. S1. ^{1}H NMR spectrum of **L1** in $CDCl_3$.

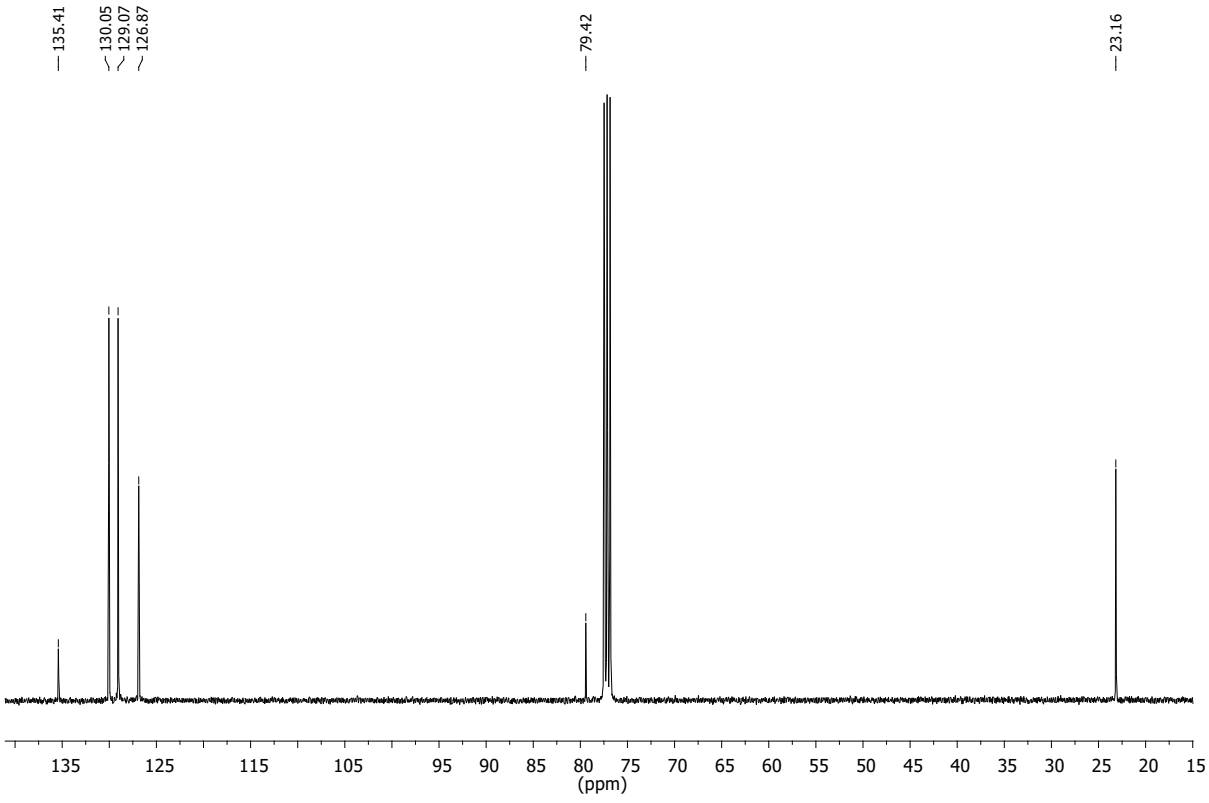

Fig. S2. $^{13}C\{^{1}H\}$ NMR spectrum of **L1** in $CDCl_3$.

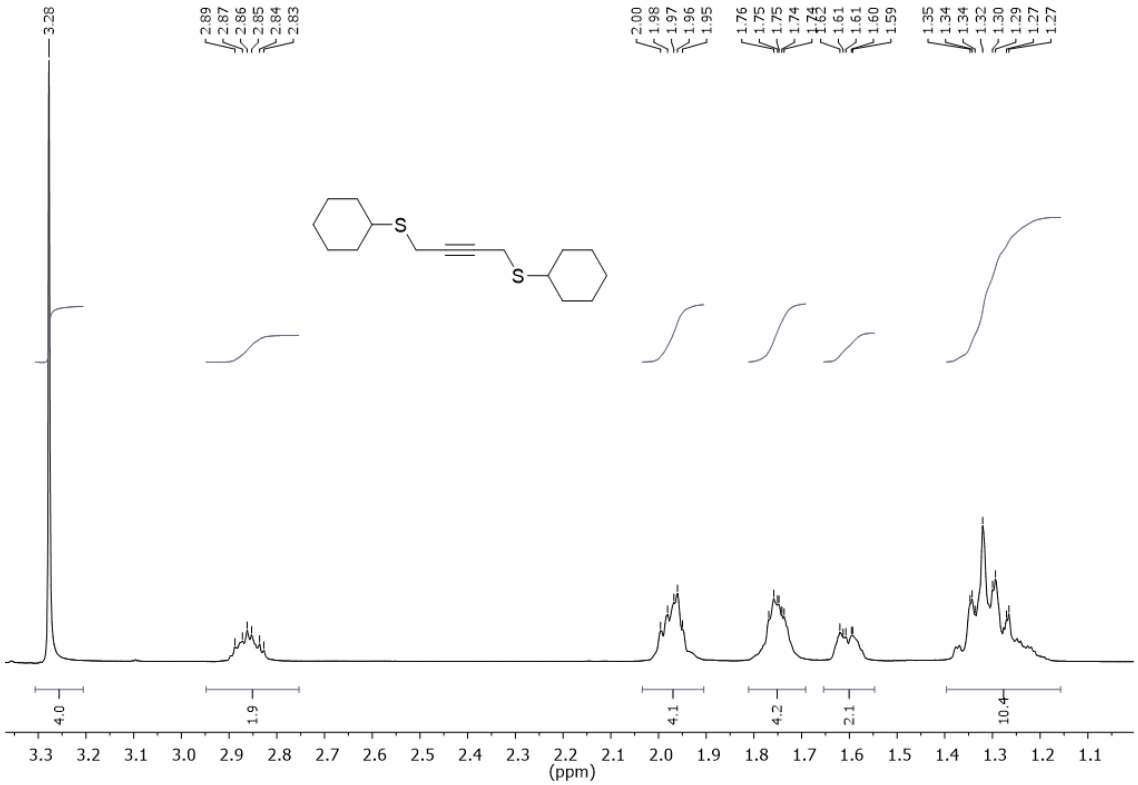

Fig. S3. ^{1}H NMR spectrum of **L2** in $CDCl_3$.

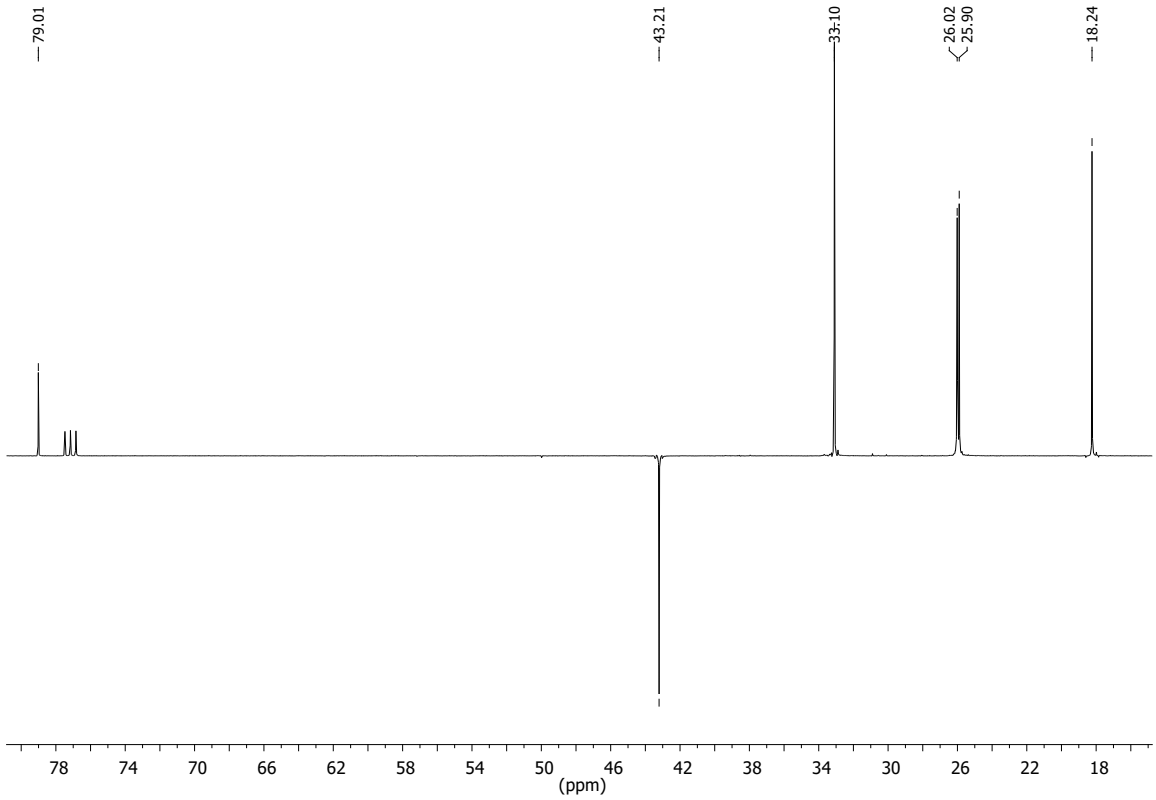

Fig. S4. $^{13}C\{^{1}H]$ J-mod spectrum of **L2** in $CDCl_3$.

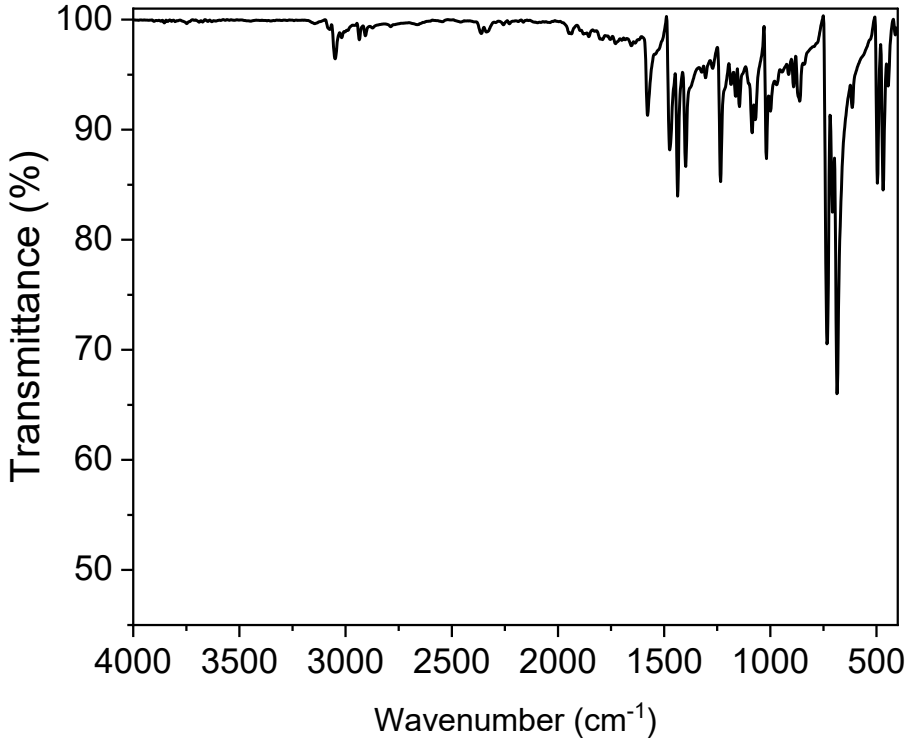

Fig. S5. ATR-IR spectrum of **L1**.

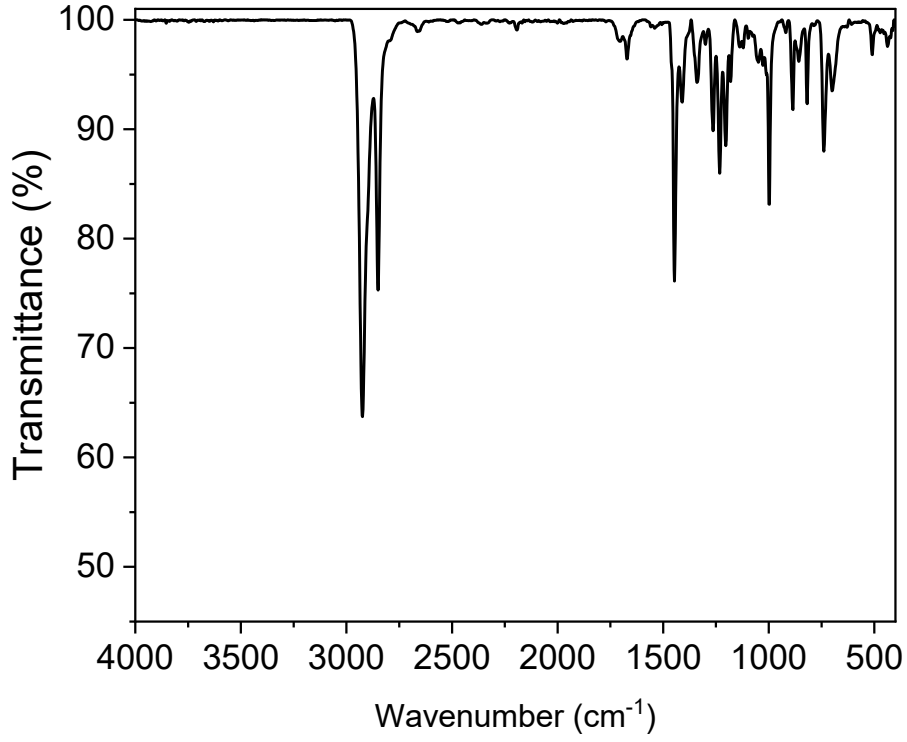

Fig. S6. ATR-IR spectrum of **L2**.

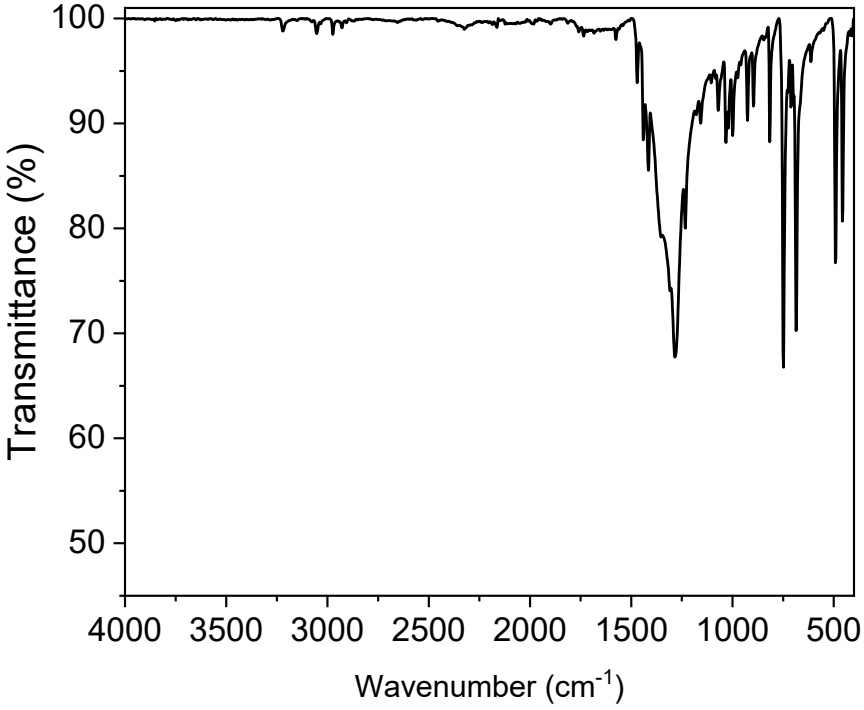

Fig. S7. ATR-IR spectrum of **CP1**.

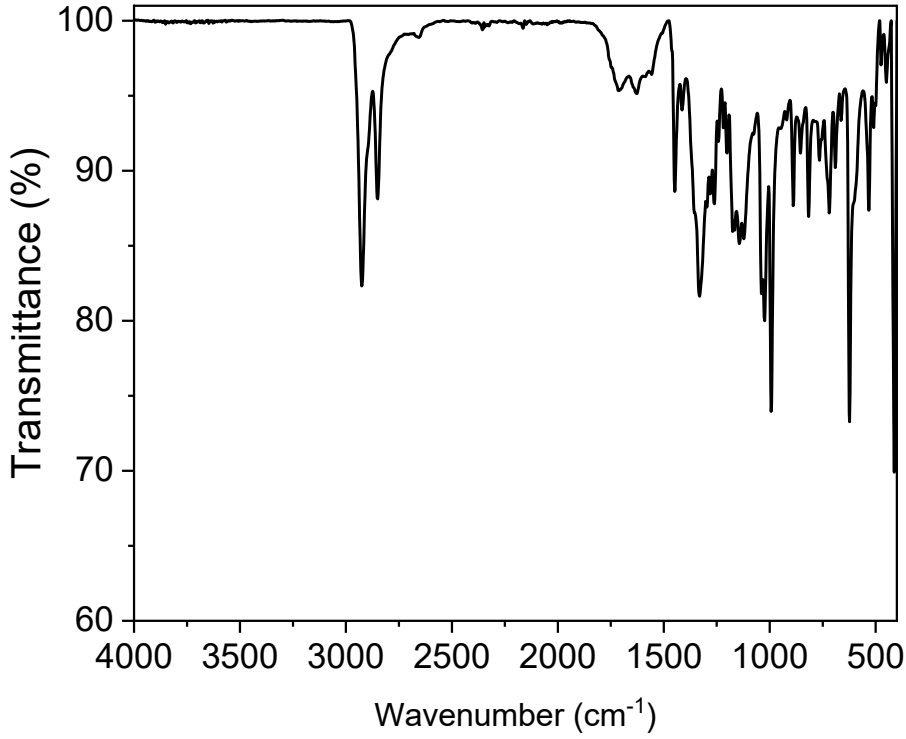

Fig. S8. ATR-IR spectrum of **CP2**.

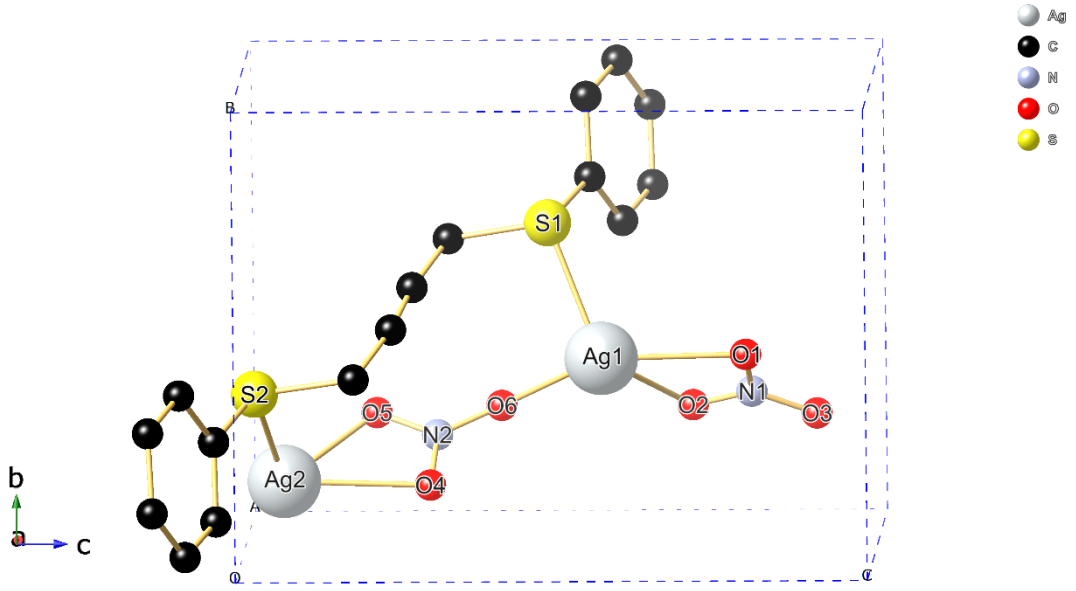

Fig. S9. Asymmetric unit of **CP1**.

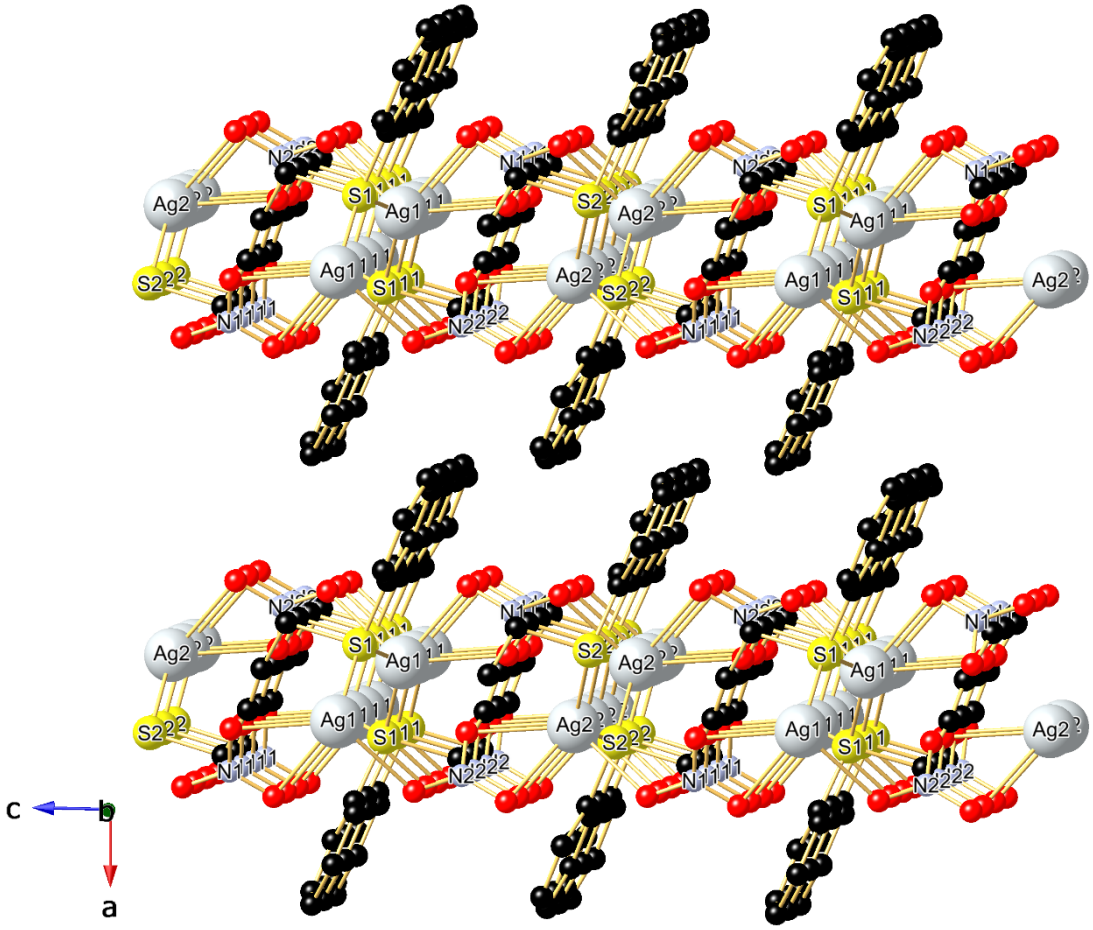

Fig. S10. View down the *c* axis of two layers of the 2D network of **CP1**.

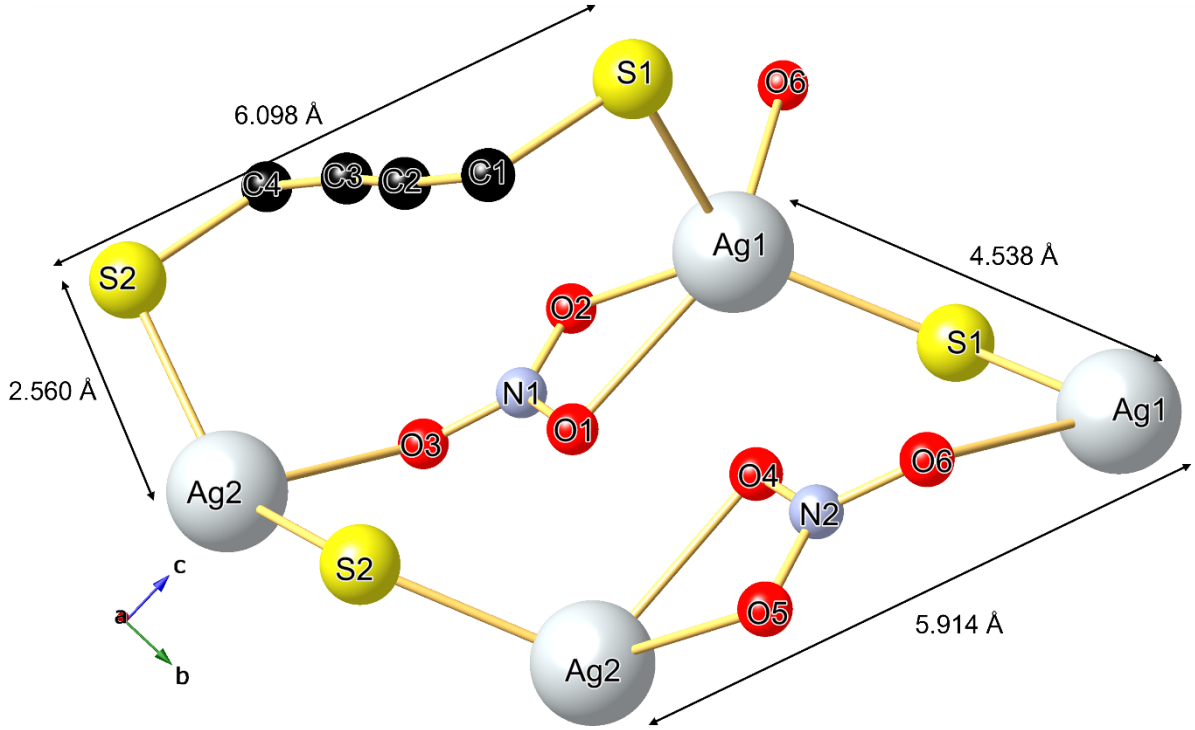

Fig. S11. View of the 11 and 12-membered parallelogram-shaped units in the 2D network of **CP1**.

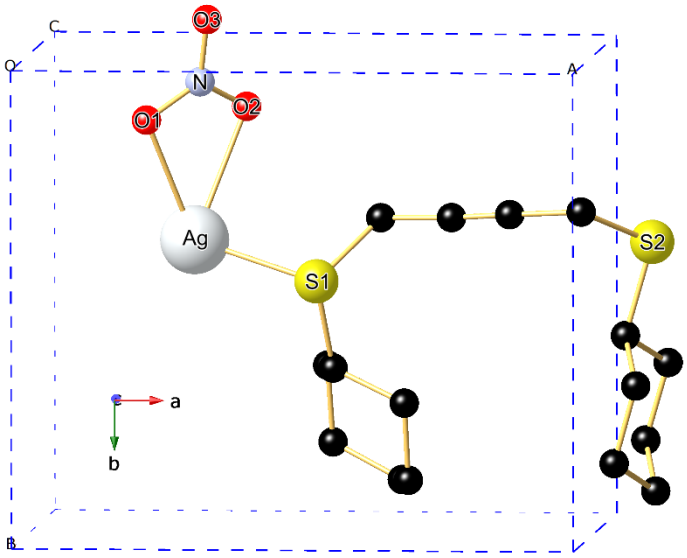

Fig. S12. Asymmetric unit of **CP2**.

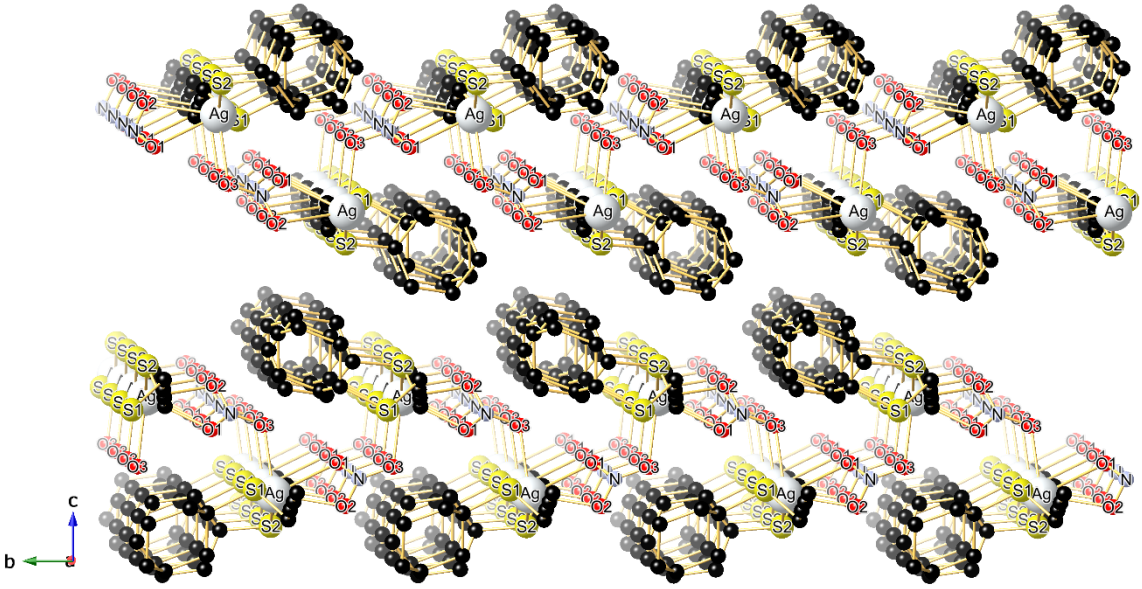

Fig. S13. View down the *a* axis of two layers of the 2D network of **CP2**.

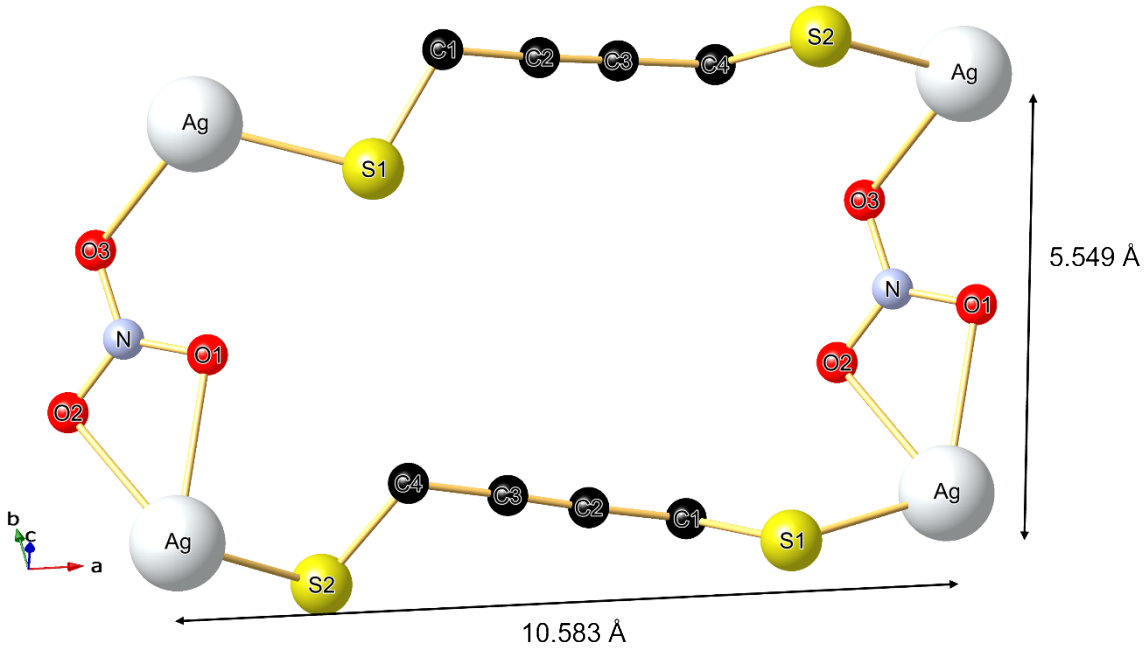

Fig. S14. View of the 22-membered parallelogram-shaped units in the 2D network of **CP2**.

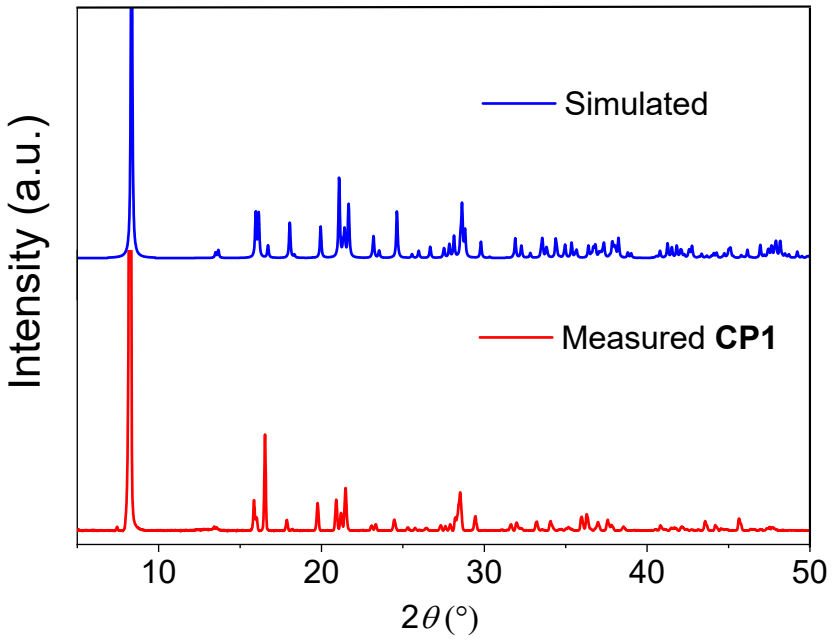

Fig. S15. Simulated and experimental PXRD of **CP1**.

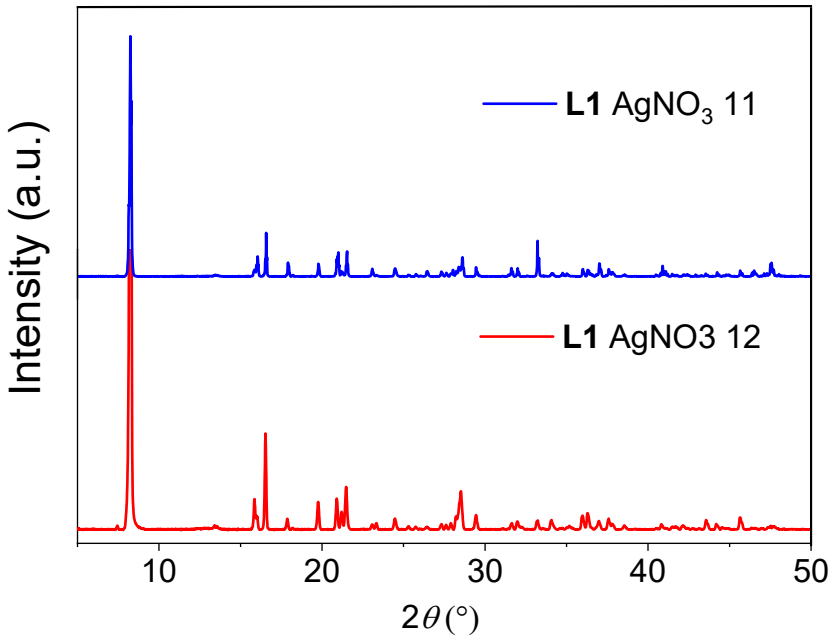

Fig. S16. Comparison of the PXRD patterns obtained using a 1:1 and a 1:2 **L1**:$AgNO_3$ ratios.

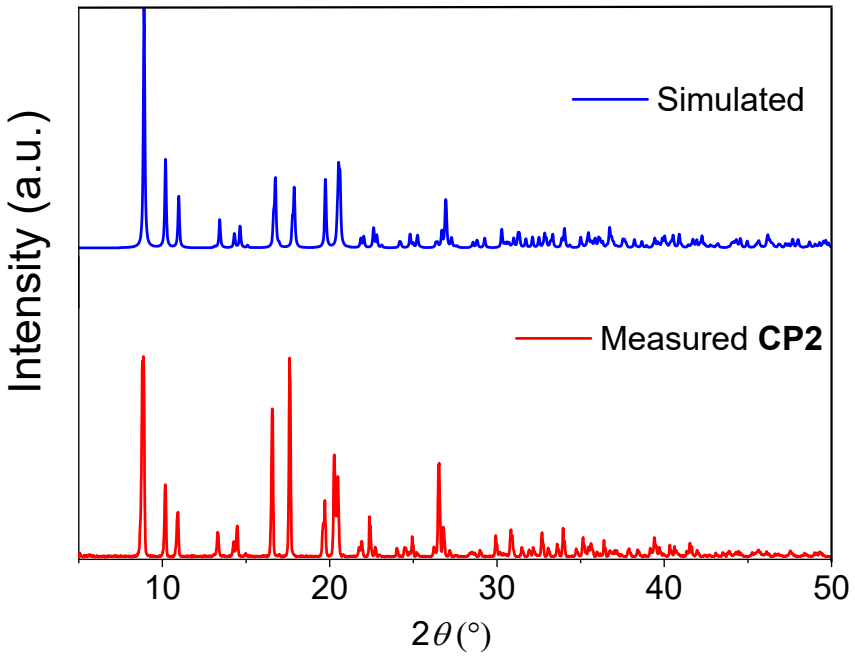

Fig. S17. Simulated and experimental PXRD of **CP2**.

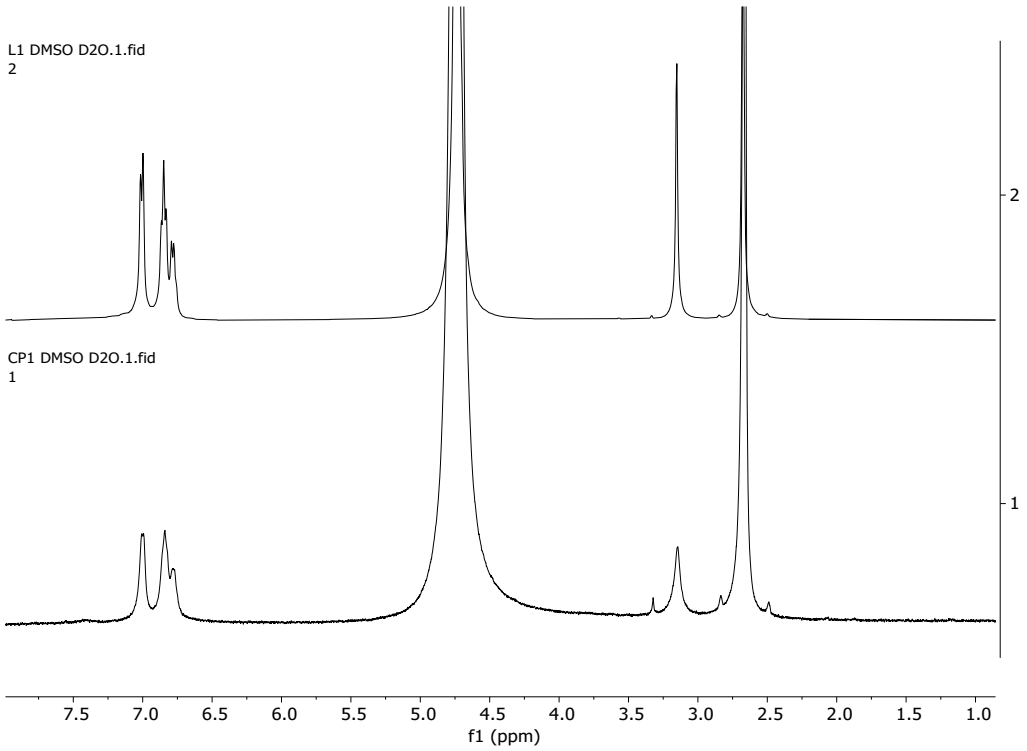

Fig. S18. Comparison of ^{1}H NMR spectra of **L1** and **CP1** in 20% DMSO-d_6/D_2O solution.

Table S1. Crystal data, data collection, and structure refinement for **CP1** and **CP2**.

Compound	**CP1**	**CP2**
Formula	$C_{16}H_{14}Ag_2N_2O_6S_2$	$C_{16}H_{26}AgNO_3S_2$
Formula weight	610.15	452.37
Temperature/K	100	100
Wavelength/Å	0.71073	0.71073
Crystal system	monoclinic	monoclinic
Space group	$P2_1$	$P2_1/n$
a/Å	10.5968(6)	10.5832(5)
b/Å	8.2082(5)	8.8168(7)
c/Å	10.9599(6)	20.0863(17)
α/°	90	90
β/°	91.200(2)	99.314(3)
γ/°	90	90
Volume/ Å^3	953.09(9)	1849.5(2)
Z	2	4
Density (calc.) g/cm^3	2.126	1.625
Absorption coefficient/mm^{-1}	2.311	1.328
F(000)	596.0	928.0
Crystal size/mm	0.437 × 0.381 × 0.16	0.373 × 0.137 × 0.066
2θ range for data collection/°	3.716 to 72.546	6.048 to 79.998
Index ranges	-17 ≤ h ≤ 17, -13 ≤ k ≤ 13, -18 ≤ l ≤ 18	-19 ≤ h ≤ 19, -15 ≤ k ≤ 15, -36 ≤ l ≤ 36
Reflections collected	74051	55509
Independent reflections	9215 [R_{int} = 0.0286, R_{sigma} = 0.0163]	11428 [R_{int} = 0.0305, R_{sigma} = 0.0241]
Refinement method	Full-matrix least-squares on F^2	Full-matrix least-squares on F^2
Data / restraints / parameters	9215/1/254	11428/0/208
Goodness-of-fit on F^2	1.202	1.042
Final *R* indices [I>2σ(I)]	R_1 = 0.0257, wR_2 = 0.0522	R_1 = 0.0219, wR_2 = 0.0497
R indices (all data)	R_1 = 0.0279, wR_2 = 0.0538	R_1 = 0.0275, wR_2 = 0.0529
Largest diff. peak and hole/e. Å^{-3}	2.41/-1.78	0.55/-0.55

Table S2. Selected bond lengths (Å) and angles (°) of **CP1** at 100K

atom1 – atom2	Distance (Å)	atom1 – atom2- atom3	Angle (°)
Ag1–S1[1]	2.5704(12)	S1–Ag1–S1[1]	133.64(2)
Ag1–S1	2.5346(12)	S1[1]–Ag1–O1	104.04(12)
Ag2–S2	2.5486(13)	S1–Ag1–O1	109.76(14)
Ag2–S2[2]	2.5601(14)	S1[1]–Ag1–O2	108.40(11)
Ag1–O1	2.502(4)	S1–Ag1–O2	117.46(11)
Ag1–O2	2.561(5)	S1[1]–Ag1–O6	92.70(10)
Ag1–O6	2.638(4)	S1–Ag1–O6	89.57(11)
Ag2–O3[3]	2.596(4)	O1–Ag1–O2	50.46(13)
Ag2–O4	2.532(4)	O1–Ag1–O6	129.53(13)
Ag2–O5	2.549(4)	O2–Ag1–O6	79.12(12)
O1–N1	1.264(6)	S2–Ag2–S2[2]	133.14(2)
O2–N1	1.239(5)	S2–Ag2–O3[3]	94.44(11)
O3–N1	1.253(5)	S2[2]–Ag1–O3[3]	90.56(11)
O4–N2	1.264(6)	S2–Ag2–O4	103.89(14)
O5–N2	1.270(5)	S2[2]–Ag2–O4	107.42(15)
O6–N2	1.254(6)	S2–Ag2–O5	109.56(11)
		S2[2]–Ag2–O5	117.21(11)
		O3[3]–Ag2–O4	130.99(13)
		O3[3]–Ag2–O5	80.48(12)
		O4–Ag2–O5	50.62(12)

Symmetry transformations used to generate equivalent atoms: [1]1-*x*, -1/2+y, 1-z; [2]1-x, -1/2+y, -z; [3]+x, +y, -1+z.

Table S3. Selected bond lengths (Å) and angles (°) of **CP2** at 100K

atom1 – atom2	Distance (Å)	atom1 – atom2- atom3	Angle (°)
Ag–S1	2.4652(2)	S1–Ag1–S2[1]	151.607(7)
Ag–S2[1]	2.4833(2)	S1–Ag1–O1	118.364(17)
Ag–O1	2.5798(7)	S1–Ag1–O2	88.249(18)
Ag–O2	2.6411(8)	S1–Ag1–O3[2]	103.692(16)
Ag–O3[2]	2.5726(7)	S2[1]–Ag1–O1	88.309(17)
O1–N1	1.2539(9)	S2[1]–Ag1–O2	104.387(19)
O2–N1	1.2547(10)	S2[1]–Ag1–O3[2]	95.117(17)
O3[2]–N1	1.2536(9)	O1–Ag1–O2	49.04(2)
		O1–Ag1–O3[2]	67.67(2)
		O2–Ag1–O3[2]	111.92(2)

Symmetry transformations used to generate equivalent atoms: [1-]1+*x*, +*y*, +*z*; [2]1/2-x, 1/2+y, 1/2-z.

Table S4. Comparison of Ag–S and Ag–O bond distances found in 2D CPs prepared by coordination of dithioether ligands with $AgNO_3$.

References CSD	Ligand	Reference	Ag–S (Å)	Ag–O (Å)
FAZPUS	$PhSCH_2C{=}CCH_2SPh$	5	2.540-2.583	2.440-2.547
VEDWIL	$PhS(CH_2)_{10}SPh$	6	2.494- 2.512	2.461-2.491
XOLPAP	$PhS(CH_2)_4SPh$	7	2.534-2.557	2.452-2.577
HOSSIS	$CySCH_2PhCH_2SCy$	8	2.4699-2.5108	2.415-2.516
CP2	$CySCH_2C{\equiv}CCH_2SCy$	This work	2.4652-2.4833	2.5726-2.6411

7. References

1. F. R. Hartley, S. G. Murray, W. Leavson, H. E. Soutter and C. A. McAuliffe, *Inorg. Chim. Acta*, **1979**, *35*, 265-277.
2. O. V. Dolomanov, L. J. Bourhis, R. J. Gildea, J. A. K. Howard, H. Puschmann, *J. Appl. Cryst.* **2009**, *42*, 339–341.
3. G. M. Sheldrick 2015. *Acta Cryst*. **2015**, *A71*, 3–8.
4. G. M. Sheldrick 2015. *Acta Cryst*. **2015**, *C71*, 3–8.
5. Y. Zheng, J.-R. Li, M. Du, R.-Q. Zou and X.-H. Bu, *Crystal Growth & Design*, 2005, **5**, 215-222.
6. M. O. Awaleh, A. Badia, F. Brisse and X.-H. Bu, *Inorg. Chem.*, 2006, **45**, 1560-1574.
7. X.-H. Bu, W. Chen, W.-F. Hou, M. Du, R.-H. Zhang and F. Brisse, *Inorg. Chem.*, 2002, **41**, 3477-3482.
8. T. H. Kim, Y. W. Shin, K.-M. Park and J. Kim, *Acta Cryst. E*, 2009, **65**, m385.